11th International Symposium on Turbulence and Shear Flow Phenomena (TSFP11)
Southampton, UK, July 30 to August 2, 2019

A PARTICLE-RESOLVED DIRECT-NUMERICAL SIMULATION STUDY OF PARTICLE-LADEN TURBULENT CHANNEL FLOW USING A MASSIVELY PARALLEL, UNSTRUCTURED, OVERSET METHOD

Wyatt Horne
Department of Aerospace Engineering and Mechanics...
University of Minnesota
110 Union St SE, Minneapolis, MN 55455
horne070@umn.edu

Krishnan Mahesh
Department of Aerospace Engineering and Mechanics
University of Minnesota
110 Union St SE, Minneapolis, MN 55455
kmahesh@umn.edu

ABSTRACT

Particle-laden, turbulent fluid flows often feature a large range of length scales spanning from large convective scales down to scales below that of individual particles. Particle-resolved direct-numerical simulations (PR-DNS) seek to resolve all scales present in particle-laden flow using first principal approaches Tenneti & Subramaniam (2014). Resolving the fluid features at and below that of individual particles for cases with many, moving particles presents difficult numerical challenges. In this work, unstructured meshes are attached to moving particles and placed within a fixed background domain. A dynamic overset assembly calculation is performed to connect the fluid flow solutions between the overlapping meshes. An incompressible, high-resolution, finite-volume method is used to solve for the fluid flow. Particle hydrodynamic forces are directly integrated along particle surfaces to provide rigid-body motion. The method scales to large numbers of particles, O(10,000-100,000), while also providing high resolution near the particle surfaces and solid boundaries of the domain. Using this approach, simulations of particle-laden channel flow are performed. Inertial particles are selected which can exhibit non-trivial particle slip-velocity near the channel walls Li *et al.* (2001*b*). Flow and particle statistics and flow fields are presented for the case of 10,000 and 50,000 particles in $Re = 180$ channel flow.

Introduction

Turbulent particle-laden flows are commonly found in engineering applications and nature such as in gas-turbine aircraft engines, solid-particle solar receivers, and particulate transport in the atmosphere Mcleod *et al.* (1999); Meher-Homji & Bromley (2004); Chen *et al.* (2007*a*); Kok *et al.* (2012); Chen *et al.* (2007*b*). There is much uncertainty in predicting the physics of such systems. For example, in the Climate Change Conference in 2014, Pachauri *et al.* (2014), it was found that the largest uncertainty present in climate forcing calculations for Earth was due to particulates in the atmosphere. Understanding the physics of particle-laden turbulent flow is crucial to reducing this uncertainty. One way to reduce the uncertainty in the predictions of turbulent particle-laden flows is through the use of Particle-Resolved Direct Numerical Simulations (PR-DNS). In such simulations the fluid flow is resolved well beneath the scales of individual particles. Hydrodynamic forces are directly integrated along the particle surfaces to provide motion with time. This drastically reduces the uncertainty in results from the calculations relative to other methods, such as Euler-Lagrangian (E-L), or Euler-Euler (E-E) methods, which employ empirical models to move particles within the simulation.

Methods to perform PR-DNS can be broadly placed within two categories, non-conforming methods and body-fitted methods. In non-conforming methods, particle surfaces move along a non-conforming, typically Cartesian, fluid domain mesh. Forces and constrained are applied to the Cartesian fluid mesh which yield the desired moving boundary conditions. IBM is an example of a non-conforming method which has been used to perform PR-DNS of turbulent particle-laden flow. In IBM a force is added to the governing equations which yields the desired non-conforming boundary conditions. This is relatively efficient and is generally easier to implement relative to a body-fitted method, e.g. Patankar *et al.* (2001); Choi & Joseph (2001). One disadvantage of IBM is the necessity of high resolution in the vicinity of moving boundaries, especially for high Reynolds numbers (*Re*) (Iaccarino & Verzicco, 2003; Yang, 2014). Resolution must be placed in locations near moving boundaries, which are often unknown, or the mesh must be adaptively refined near the moving boundaries which has similar disadvantages to body-fitted methods. Often in place of adaptive refinement, the entire Cartesian mesh is set to an adequate resolution to resolve the particles. This results in large, non-optimal meshes with unnecessarily high resolution over much of the domain.

In body-fitted methods it is possible to ensure adequate resolution at the surfaces of moving bodies with conforming meshes. If an overset methodology is used, it is possible to avoid the necessity of adaptive mesh refinement or large, non-optimal meshes. In an overset method meshes are directly attached to surfaces and allowed to arbitrarily overlap and move throughout the solution domain (Wang & Parthasarathy, 2000; Meakin & Suhs, 1989). A key challenge of an overset method is connecting the solution between meshes robustly, efficiently, and accurately throughout the domain. Mesh cells can be located exterior to the solution domain and must be removed from the solution. Additionally, there may be region of the domain where may meshes overlap and redundant solutions exist. For best efficiency, cells within these regions must be selectively removed to reduce the redundancy while covering the entire domain. Boundaries remain at the edges of overset meshes and regions of removed cells which must be supplied boundary conditions reconstructed from other meshes.

Overset and body-fitted methods in general have seen limited application to PR-DNS. The number of particles is generally low and the cases studied are relatively simple compared to what has been achieved by non-conforming methods. One reason is the inherent difficulty in scaling up the necessary connectivity calculations for overset to large numbers of meshes and computational cores. In our recent work, an overset assembly method was developed to address this issue (Horne & Mahesh, 2019*b*). The method was shown to be capable of performing connectivity calculations for large numbers of meshes on large numbers of cores. In particular, strong-scaling was demonstrated for 100,000 spherical particles moving within a turbulent channel flow up to 492,000 processors.

Another difficulty in overset methods is the presence of conservation and interpolation error, especially when many overlapping meshes are present at differing resolutions. In our recent work, a supercell reconstruction was presented which allows for accurate, energy bounded reconstruction between meshes without increasing computational stencils. For mass conservation, a penalty based method which weakly enforces boundary conditions between mesh was presented. This method allows for global mass conservation while producing linear systems that are symmetric and positive-definite such that they are efficiently solved using modern matrix inversion techniques (Horne & Mahesh, 2019*a*).

In this work, we apply the unstructured overset method described in Horne & Mahesh (2019*a*,*b*) to the case of turbulent particle laden vertical channel flow. The flow can exhibit rich, challenging-to-predict physics such as turbulence attenuation, preferential concentration, and particle accumulation (Kulick *et al.*, 1994). First the overset assembly and numerical methods will be overviewed. Then the case and simulation domain will be overviewed, followed by a presentation and discussion of the simulation results.

Overset Assembly and Numerical Methods

Multiple meshes are placed within a domain and allowed to arbitrarily overlap when performing an overset simulation. The solutions between the different meshes are connected through an overset assembly process. Using the method described in (Horne & Mahesh, 2019*b*), Fig. (1) depicts the assembly process for a spherical particle at a wall. During a simulation, control volumes are dynamically found outside the solution domain, shown in the red region in the figure, and must be removed from the simulation dynamically as particles move. Redundant solutions can be present depending on mesh overlap. Control volumes within these regions are selectively removed as much as possible for improved efficiency. After the removal of control volumes, exposed surfaces remain which must be provided boundary conditions. The solutions from overlapping meshes provide these boundary conditions through reconstructions or constraints.

The motion of the fluid phase is modeled using the incompressible Navier-Stokes equations. For movement, an arbitrary Lagrangian-Eulerian (ALE) formulation of the equations is used. The ALE formulation avoids tracking multiple reference frames for arbitrary motion of meshes through the inclusion of the mesh velocity in the convection term.

$$\int_\Omega \frac{\partial u_i}{\partial t} dV + \int_{\partial\Omega} (u_i (u^n - u^n_{mesh}) dA) = -\int_\Omega \frac{1}{\rho} \frac{\partial p}{\partial x_i} dV + \int_{\partial\Omega} \nu \frac{\partial u_i}{\partial n} dA \tag{1}$$

$$\int_{\partial\Omega} u^n dA = 0 \tag{2}$$

The equations are integrated over control volume Ω, with faces $\partial\Omega$ which have normals n. Here, u_i is the inertial fluid velocity in the ith Cartesian direction, u^n is the inertial velocity normal to the faces of the control volume, u^n_{mesh} is the velocity of the mesh normal to the faces of the control volume, p is the pressure, and ρ is the fluid density. To discretize these equations a non-dissipative, high resolution, unstructured finite volume scheme which focuses on kinetic energy conservation, as shown in Horne & Mahesh (2019*a*), is used. The method is a predictor-corrector formulation, requiring reconstructions at overset boundaries for the predicted velocity and corrector pressure steps. A supercell reconstruction is used for both of these steps which coarsens solutions to match differing mesh resolutions. For predicted velocity, the reconstruction is placed directly into the linear system. For pressure, a penalty formulation is used which adds a penalty force to the overset boundaries to yield the reconstructed values at the boundary.

Hydrodynamic forces are directly integrated along the particle surfaces using the fluid phase solution. Euler's equations of solid body motion are then solved in each particle's body frame of reference. Quaternions are used to represent the rotational orientation of the particles. Quaternions are four vectors which provide orientation information in a frame universal manner. Quaternions offer several advantages to other rotation orientation representations, such as Euler angles. They do not require any trigonometric calculations, are generally more compact, vary smoothly in rotational space, and avoid gimbal locking (Wertz, 1980). The formulation used in this work retains these properties and also avoids the need to recalculate any angular properties over time since the equations are defined in principal orthogonal coordinates. Additionally, complex rotational motions such as precession can be directly captured using the formulation.

Collisions between particles is a common feature in fluid flows of interest to PR-DNS. In the present work a linear spring-damper model is used for solid-solid body contact. This selection has been found by other work on PR-

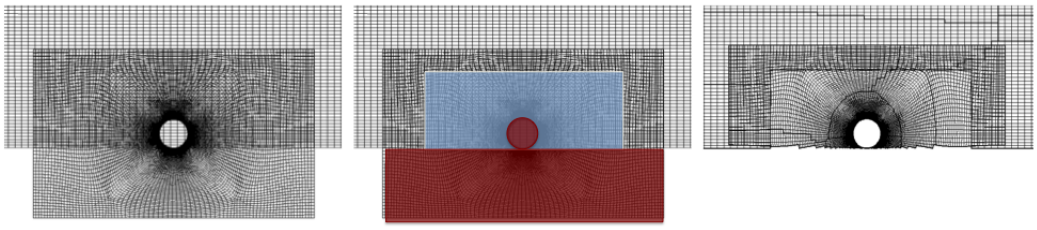

Figure 1. Spherical particle near wall overset example before and after cutting using an angled rectangular box primitive shape from Horne & Mahesh (2019*b*). Blue (■) regions indicate a region where overlap must be reduced. Red (■) regions indicate elements that lie within solid boundaries. Note that elements on the background channel mesh within the particle and (■) are removed and elements on the particle mesh below the channel wall are removed.

DNS to produce accurate results for cases with collisions (Kidanemariam & Uhlmann, 2014; Costa *et al.*, 2015). In general collisional time scales are much shorter than fluid flow time scales. If the fluid flow is advanced at the collisional time scales, simulations become quickly intractable. If the motion of particles are rapidly changed within a fluid flow time step, the resulting fluid motion can potentially be numerically unstable. In the present method, similar to the work of Costa *et al.* (2015), collisions are stretched over a fixed, specified number of time steps. This was demonstrated to produce accurate results for spherical particle collisions in Horne & Mahesh (2019*a*).

Simulation Setup

Simulations are performed of 10,000 and 50,000 spherical particles in a turbulent vertical channel. Preliminary simulations were performed to select mesh resolutions. Meshes were uniformly refined until mean flow velocity statistics had converged within 1%.

The domain and mesh information is give in Table. (1). Spherical particles chosen with diameter D_p. L_x is the length of the domain with N_x control volumes in a given direction, D_p/Δ_{bg} is the number of control volumes per diameter on the uniform background channel mesh, $N_{o,vol}$ is the number of control volumes on each overset mesh, D_p/Δ_e is the number of control volumes per diameter at the edge of each overset mesh, and D_p/Δ_s is the number of control volumes per diameter near the surfaces of the particles.

The particle Stokes number, Stk, particle-to-fluid density ratio, m^*, particle mass loading M, and particle volumetric loading V play significant roles in the motion of the fluid and particles for this case. The selected parameters for this study are given in Table. (2) for 10,000 particles then 50,000 particles respectively. Heavy inertial particles are selected at a relatively high value of Stokes number, $Stk = 25$. These selections will result in particle motion which can substantially differ from the fluid motion. In particular, moderate particle slip-velocity is expected near the walls of the channel, as found in other work in this regime (Li *et al.*, 2001*a*; Kulick *et al.*, 1994).

A constant volumetric force is used to provide fluid flow at a friction Reynolds number of $Re_\tau = 180$. The flow is initialized with a laminar channel profile, at full Re_τ and with all initially stationary particles. Flow disturbances, necessary for the transition to turbulence, are provided by the particles.

Table 1. Channel and overset mesh information.

$L_x \times L_y \times L_z$	$N_x \times N_y \times N_z$	D_p/Δ_{bg}
$4\pi \times 2 \times \pi$	$1934 \times 616 \times 967$	4

$N_{o,vol}$	D_p/Δ_e	D_p/Δ_s	D_p
15543	4	40	0.013

Table 2. Particle and channel non-dimensional parameters

Stk	m^*	Re_τ	M	V
25	175	180	0.0255	0.00015
25	175	180	0.1275	0.00075

Results

The time-averaged and spatially averaged streamwise velocity profiles of the fluid and particles are compared to DNS of a clean channel from Moser *et al.* (1999) in Fig. (2). The fluid velocity is found to reasonably match the clean channel flow result. The particle concentrations here are dilute such that statistical differences in the mean streamwise velocity will be negligible. The average particle velocity is found to be significantly higher than the fluid velocity near the wall. Additionally, the particles are found to be slower than the fluid near the center of the channel. Overall the average particle Reynolds number ranges from $Re = 0 - 10.4$. To simulate this case using a point particle, or two fluid method, one would have to include particle dynamics which include significant particle slip velocities.

The average Reynolds stresses of the fluid are compared to a clean channel result in Fig. (3) for 10,000 particles in the channel. Unlike the streamwise velocity, significant deviations from the clean channel are found. The turbulent kinetic energy is found to be relatively less near the wall when particles are present, mostly due to the decreased values of $\overline{u'u'}$ near the wall. It has been noted in past work that particle-wall collisions can significantly modify turbulent dissipation in wall-bounded flows (Li *et al.*, 2001*a*; Kulick *et al.*, 1994). There is a high occurrence of particle collisions with the channel walls, as shown in the collision PDF depicted in Fig. (4). It is likely that the high occurrence of particle-wall collision is causing the decrease in turbulent kinetic energy in the present results. It is also found that $\overline{u'u'}$ is relatively higher than the clean channel flow away from the walls. The particles are moving relatively faster than the fluid in these locations, leaving wakes in the fluid. It

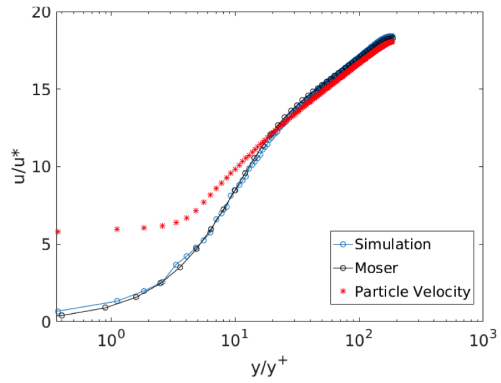

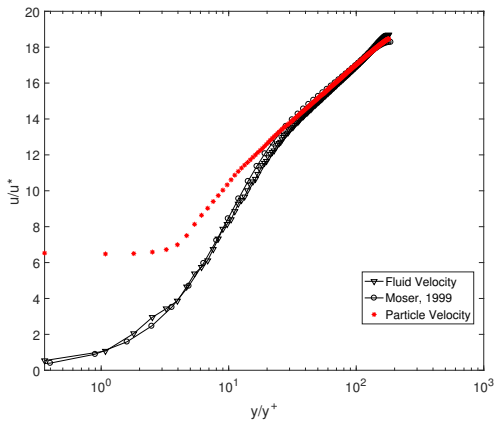

Figure 2. Average streamwise velocity of the fluid and particles compared to clean channel flow from Moser *et al.* (1999) for 10,000 particles then 50,000 particles respectively.

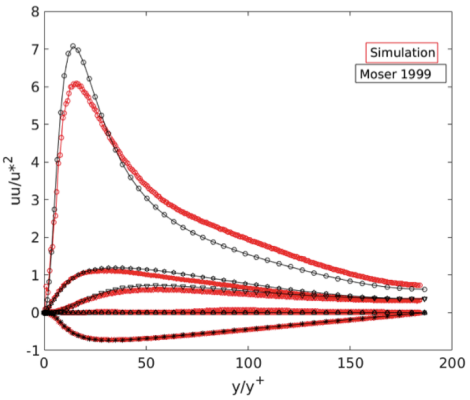

Figure 3. Average fluid Reynolds stress from the 10,000 particles simulation compared to clean channel flow from Moser *et al.* (1999).

is possible that the presence of particle wakes and particle flow disturbances lead to an increase in $\overline{u'u'}$ away from the walls.

The average wall normal locations of particles are shown in Fig. (5). The particles are found to be evenly dispersed in the center of the channel and concentrated near the channel walls. This same result has been found in experi-

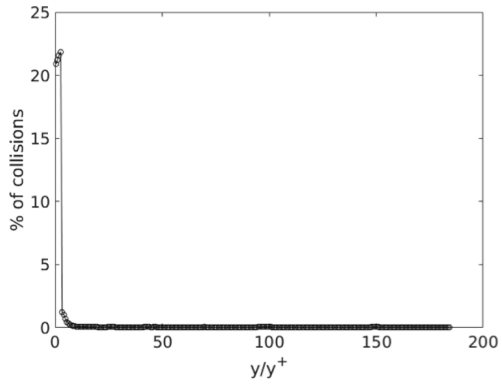

Figure 4. Occurrence of collisions throughout the channel with 10,000 particles.

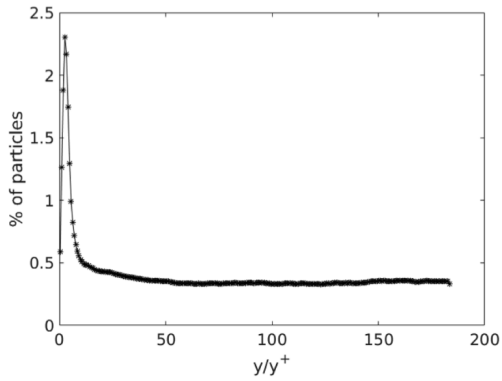

Figure 5. Particle locations throughout channel with 10,000 particles.

ments of particle-laden channel flow (Kulick *et al.*, 1994). Instantaneous flow fields of Q-criterion with particle surfaces and velocity contours are shown in fig. (6). The particles are found to be relatively dispersed throughout the channel and to not exhibit noticeable preferential concentration based on the vortex locations. Particle wakes are found in the result for particles near the center of the channel as noted before.

Conclusions

The fluid flow and particle results from the overset simulations show substantial deviations from a clean channel flow with one-way coupled point particles. The particles are found to have significant slip-velocities resulting in non-trivial particle Reynolds numbers. Particle wakes and disturbances are clearly found in the results resulting in attenuation of turbulence flow statistics. This is particularly found in $\overline{u'u'}$ where a suppression is found near the wall with heightened values occurring towards the center of the channel. Particle-wall collisions likely play an important role in the results shown. The particle and fluid statistics show a strong influence from the collisions. In particular, it has been found in previous numerical simulations of particle-laden channel flow that particles largely aggregate near walls when collisions are not fully considered (Li *et al.*,

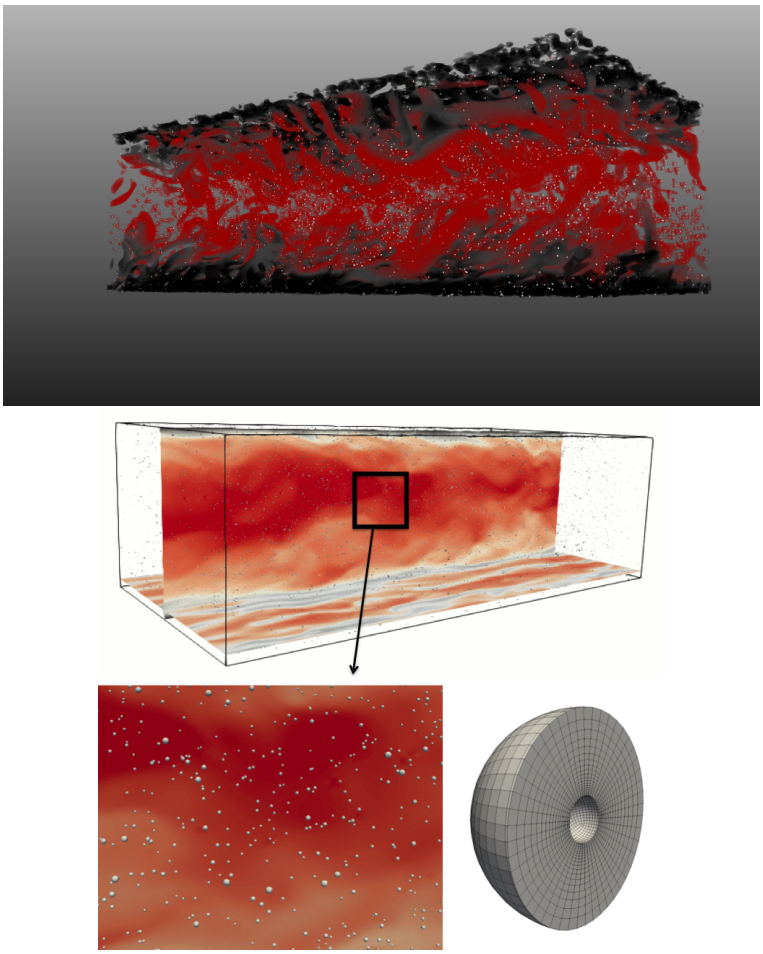

Figure 6. Iso-volumes of Q-criterion colored by streamwise velocity with particle surfaces for 10,000 particles followed by instantaneous velocity contours with particle surfaces for 50,000 particles. Each surface in the shown results has the shown mesh attached to it.

2001*a*). When collisions are included, particles are found at relatively decreased concentrations near the wall with a uniform concentration in the center of the channel. The results for particle location shown here match this description.

Acknowledgments

The work was made possible by support under the Predictive Academic Alliance Program (PSAAP2) through the Department of Energy under DE-NA0002373. Computational resources were provided by Argonne National Laboratory. Further resources for this work were provided by the National Science Foundation (NSF) under NSF Grant CBET-1510154.

REFERENCES

Chen, H., Chen, Y., Hsieh, H-T. & Siegel, N. 2007*a* Computational fluid dynamics modeling of gas-particle flow within a solid-particle solar receiver. *Journal of solar energy engineering* **129** (2), 160–170.

Chen, H., Chen, Y., Hsieh, H. T. & Siegel, N. 2007*b* Computational fluid dynamics modeling of gas-particle flow within a solid-particle solar receiver. *Journal of Solar Energy Engineering* **129**.

Choi, H.G. & Joseph, D.D. 2001 Fluidization of 300 circular particles in plane poiseuille flow by direct numerical simulation. *Journal of Fluid Mechanics* **438**, 101–128.

Costa, P., Boersma, B.J., Westerweel, J. & Bruegem, W-P. 2015 Collision model for fully resolved simulations of flows laden with finite sized particles. *Physical Review E* **92**, 053012.

Horne, Wyatt James & Mahesh, Krishnan 2019*a* A conservative massively-parallel overset method for simulating fluid flow over moving bodies. *Journal of Computational Physics* **Submitted**.

Horne, Wyatt James & Mahesh, Krishnan 2019*b* A massively-parallel, unstructured overset method for mesh connectivity. *Journal of Computational Physics* **376**, 585–596.

Iaccarino, G. & Verzicco, R. 2003 Immersed boundary technique for turbulent flow simulations. *Applied Mechanics Review* **56**, 331–347.

Kidanemariam, A.G. & Uhlmann, M. 2014 Interface-resolved direct numerical simulation of the erosion of a sediment bed sheared by laminar channel flow. *International Journal of Multiphase Flow* **67**, 174–188.

Kok, J., Parteli, E., Michaels, T. & Karam, D. 2012 The physics of wind-blow sand and dust. *Reports on Progress in Physics* **75**.

Kulick, Jonathan D, Fessler, John R & Eaton, John K 1994 Particle response and turbulence modification in fully developed channel flow. *Journal of Fluid Mechanics* **277**,

109–134.

Li, Y., McLaughlin, J., Kontomaris, K. & Portela, L. 2001*a* Numerical simulation of particle-laden turbulent channel flow. *Physics of Fluids* **13** (10), 2957–2967.

Li, Yiming, McLaughlin, John B, Kontomaris, K & Portela, L 2001*b* Numerical simulation of particle-laden turbulent channel flow. *Physics of Fluids* **13** (10), 2957–2967.

Mcleod, P., Carey, S. & Sparks, R. S. J. 1999 Behaviour of particle-laden flows into the ocean: experimental simulation and geological implications. *Sedimentology* **46**, 523–536.

Meakin, R.L. & Suhs, N.E. 1989 Unsteady aerodynamic simulation of multiple bodies in relative motion. *AIAA Paper* **98**, 1996.

Meher-Homji, C.B. & Bromley, A. 2004 Gas turbine axial compressor fouling and washing. In *Proceedings of the 33rd Turbomachinery Symposium*. Texas A&M University. Turbomachinery Laboratories.

Moser, R. D., Kim, J. & Mansour, N. N. 1999 Direct numerical simulation of turbulent channel flow up to $Re_\tau = 590$. *Physics of Fluids* **11**, 943–945.

Pachauri, R., Allen, M., Barros, V., Broome, J., Cramer, W., Christ, R., Church, J., Clarke, L., Dahe, Q. & Dasgupta, P. 2014 *Climate change 2014: synthesis report. Contribution of Working Groups I, II and III to the fifth assessment report of the Intergovernmental Panel on Climate Change*. IPCC.

Patankar, N.A., Huang, P.Y., Ko, T. & Joseph, D.D. 2001 Lift-off of a single particle in newtonian and viscoelastic fluids by direct simulation. *Journal of Fluid Mechanics* **438**, 7–100.

Tenneti, S. & Subramaniam, S. 2014 Particle-resolved direct numerical simulation for gas-solid flow model development. *Annual Review of Fluid Mechanics* **46**, 199–230.

Wang, Z.J. & Parthasarathy, V. 2000 A fully automated chimera methodology for multiple moving body problems. *International Journal for Numerical Methods in Fluids* **33**, 919–938.

Wertz, J. 1980 D. Reidel Publishing Company.

Yang, F. Sotiropoulos X. 2014 Immersed boundary methods for simulating fluid-structure interaction. *Progress in Aerospace Sciences* **65**, 1–21.